Journal of Physical Chemistry & Biophysics

Geetha et al., J Phys Chem Biophys 2018, 8:3
DOI: 10.4172/2161-0398.1000273

Short Communication Open Access

Synthesis and Characterization of $Lamn_{1-X}Fe_xO_3$ (X=0, 0.1, 0.2) by Coprecipitation Route

Geetha N[1], Senthil Kumar V[1] and Prakash D[2]*

[1]Department of Physics, Karpagam Academy of Higher Education, Tamil Nadu, India

[2]Department of Physics, Hindustan Institute of Technology, Tamil Nadu, India

Abstract

Perovskite type oxides are fascinating nanomaterials and its physical properties of interest to materials science through perovskites include superconductivity, magnetoresistance, ionic conductivity, and a multitude of dielectric properties, which are of great importance in microelectronics and telecommunication. Recently interest has arisen in perovskite-type oxides as catalysts due to high thermal and hydrothermal stability as well as high mechanical strength among other properties. In the present work, LaMn1-xFexO3 perovskite was synthesized by the co-precipitation method. The product was characterized by X-ray diffractometer (XRD), Scanning electron microscope (SEM), Energy dispersive X-ray spectrometer (EDX), Fourier transform infrared spectroscopy (FTIR), UV-visible absorption spectroscopy and conductivity study. The XRD pattern confirmed the formation of perovskite phase. The SEM micrographs indicated that the morphology contain porosity due to inter-particle voids. The presence of functional groups of the pure and doped lanthanum manganite were studied by FTIR. The optical band gap decreases with increasing the content of iron in the sample. The conductivity study confirmed that the conductivity increases with increasing the content of iron.

Keywords: $LaMn_{1-x}Fe_xO_3$; Co-precipitation; XRD; FTIR; Conductivity

Introduction

During the last decade there have been carried extensive searches and investigations of various oxide systems, which can be used as multifunctional materials, possessing combination of electric, dielectric, ferroelectric, ferroelastic, magnetic and other properties. Such materials can be used in different kinds of micro- and nanostructured materials of the new generation such as thin films, super lattices, nanofibers, nanotubes and nanowires [1-5]. The number of catalysts used in modern chemical industries are based on mixed oxide including perovskite oxide ABO_3 where A is a rare earth element, B is 3d transition metals remain predominant [6] perovskite oxides crystals can have broad applications in advanced technologies such as catalysts, oxide fuel cell, chemical sensors, magnetic materials, electrode materials [7-9]. Perovskites, especially $LaMnO_3$, have also been used in environmental applications, e.g., the oxidation of hydrocarbons [10-12], chlorinated organics [13] and H_2O_2 reactions [14]. $LaMnO_3$ shows good stability, flexible oxygen stoichiometry (δ) and the different Mn oxidation states i.e., Mn^{2+}, Mn^{3+}, Mn^{4+}, which strongly affects the catalytic behavior. Also, isomorphic substitution of metals in the perovskite structure allows some control the catalytic properties of the material and its several derivatives have been previously investigated [15,16]. Lanthanum-based perovskites containing transition metal in B-site, ($LaBO_3$, B=Co, Fe, Ni or Mn), show catalytic activity close to the noble metal, presenting low cost and high thermal stability. The efficiency of these materials depends on the synthesis method [17]. Many methods are available for the synthesis of perovskite oxide materials such as solid state reaction [18], sol gel [19], solution combustion synthesis, electrospinning, hydrothermal synthesis, EDTA glycine process, and reverse micro emulsion process, etc. In this work, we studied the isomorphic substitution of Mn in the $LaMnO_3$ structure by different amounts of Fe to produce $LaMn_{1-x}Fe_xO_3$. The Fe also vary the oxidation states and this property can improve the catalytic activity in oxidation processes. The sample has been prepared by co-precipitation method. The average crystallite size and morphology of the sample obtained have been investigated.

Experimental

$LaMn_{1-x}Fe_xO_3$ (x=0, 0.1, 0.2) nanoparticle were synthesized by co-precipitation method. In this method, stoichiometric amount of Lanthanum nitrate [$La(NO_3)_3.6H_2O$], Manganese chloride [$MnCl_2.4H_2O$], Ferric nitrate [$Fe(NO_3)_3.9H_2O$] were dissolved in distilled water. After complete dissolution, the solution was continuously stirred at 50°C for half an hour. Then the sodium hydroxide (NaOH) solution was slowly added until it reaches the pH is 13. After reaching this pH, the solution was continuously stirred till the black precipitate appears. The precipitate was collected by centrifugation and washed several times to remove the chloride. Then the precipitate is kept in the oven for 1 hr at 50°C. The final product was ground and kept in the muffle furnace for calcined at 800°C for 6 hoursfor removal of organic template. Synthesized perovskite sample were characterized by X-ray diffraction (XRD), scanning electron microscopy (SEM), compositional analysis (EDAX), Fourier transform infrared (FTIR), UV visible and conductivity study.

Results and Discussion

Structural analysis

The X-Ray diffraction pattern of $LaMn_{1-x}Fe_xO_3$ ($0 \le x \le 0.2$) nanoparticle were prepared at 800°C are shown in Figure 1. The XRD pattern reveals that the prepared $LaMnO_3$ (LMO) nanoparticle and iron doped $LaMnO_3$ (LMFO) nanoparticle clearly indicates their crystalline nature with the orientation along (1 1 0) and all the other peaks are indexed to the cubic (Pm3m) structure of LMO and LMFO

***Corresponding author:** Prakash D, Department of Physics, Hindustan Institute of Technology, Tamil Nadu, India, Tel: 919600840001; E-mail: prakasphy@gmail.com

Received June 14, 2018; **Accepted** June 21, 2018; **Published** June 25, 2018

Citation: Geetha N, Senthil Kumar V, Prakash D (2018) Synthesis and Characterization of $Lamn_{1-x}Fe_xO_3$ (X=0, 0.1, 0.2) by Coprecipitation Route. J Phys Chem Biophys 8: 273. doi: 10.4172/2161-0398.1000273

nanoparticles. The prepared samples exactly matched with JCPDS card no 75-0440. From the XRD pattern, the intensity of the peak increases when the iron concentration is increased. The crystallite size was calculated using Debye-Scherrer formula. The crystallite size was found to be in the range 17-20 nm. While increasing the Fe content in the sample, the crystallite size also increases simultaneously [20]. The various lattice parameters like crystallite size, dislocation density and micro strain are calculated from the XRD pattern and its values are shown in the Table 1. From the Table 1, the lattice parameter, dislocation density and strain decreases with increasing the dopant concentration. The decrease in various lattice parameters is due to the substitution of smaller ionic radii (Fe) with the larger ionic radii (La).

Morphological analysis

The surface morphology of the prepared sample was analyzed by SEM and the images for sample x=0.0, 0.1 and 0.2 are shown in Figure 2. The SEM images of undoped and 0.1 and 0.2 M of iron doped lanthanum manganite nanoparticle calcined at 800°C. Figure 2 shows the SEM images of pure and iron doped lanthanum manganite nanoparticle. These images depict that the particles possess larger agglomeration leads to the wide distribution of the sample and possibility to confirm the particle which is exhibiting a morphology tending to the spherical shape [21]. The particles of all the prepared samples are seems to be uniformly distributed. Because of the low calcination temperature of the sample, there is porosity found in the sample.

Compositional analysis

The pure and iron doped lanthanum manganite elemental compositions were carried out with the help of EDAX shown in Figure 3. From the Figure 3a, it shows the expected presence of La, Mn and O in the prepared sample and in Figure 3b and 3c confirms the stoichiometric mixture of La, Fe, Mn and O atoms in iron doped lanthanum manganite (LMFO) samples. There exists an 1% silica found in the spectra. No traces of other element were found in the spectra. The observed composition is almost equal to the initial composition of the sample taken for its preparation [22]. Table 2 represents the composition of the elements present in the samples.

FTIR analysis

FT-IR spectra were recorded in the wavenumber range from 500 to 3500 cm^{-1}. FT-IR spectra of $LaMn_{1-x}Fe_xO_3$ ($0 \le x \le 0.2$) nanoparticle are shown in Figure 4. The broad absorption band at 642 cm^{-1} in the sample is attributed to the Mn-O vibrations of MnO_6 octahedral in cubic perovskite structure [23]. With the increasing the amounts of Fe, the intensity of absorbance at 642 cm^{-1} gradually decreases. The band around 1391 and 1472 cm^{-1} are produced by bending vibrations in the bonds N-O. The sample calcined at 800°C, there are still some carbonates because of the presence of the absorption band at 855 cm^{-1} [24]. The wavenumber and corresponding assignment of vibrations were shown in Table 3.

Optical analysis

The iron doped lanthanum manganite nanoparticle prepared by co-precipitation method whose optical absorption spectra were determined in the wavelength range 200-800 nm. Figure 5a shows the absorption spectra of the prepared sample. The presence of absorption peaks seems to be at 361, 364 and 365 nm of the sample respectively [25]. The absorptions spectra reveal that, while increasing the content of iron in the sample its absorption increases proportionally. Figure 5b the tau c plot i.e., the intercept of the straight line portion of $(\alpha h\upsilon)^2$ versus ($h\upsilon$) the bandgap has been found for $LaMn_{1-x}Fe_xO_3$ ($0 \le x \le 0.2$) nanoparticle. The optical bandgap for the prepared samples were calculated and tabulated in Table 4. The values of the bandgap for $LaMn_{1-x}Fe_xO_3$ ($0 \le x \le 0.2$) nanoparticleis found to be 3.30, 3.25 and 3.24 eV. The value of the bandgap energy decreases with the increasing content of iron in the sample. This is due to the formation of newer energy levels of iron in the lanthanum manganese oxide lattice [26]. The proper replacement of lanthanum by iron sample is the best proof for the decrease in the bandgap energy.

Conductivity analysis

The dc electrical conductivity of the pure and iron doped lanthanum manganese oxide nanoparticle was performed by Keithley high resistance electrometer 6517B shown in Figure 6. In this method, initially the current was measured with respect to the applied voltage across the sample at room temperatures [27]. The sample was sandwiched between two copper electrode and annealed in an oven. The conductivity of the sample increases with the dopant concentration because of the mobility of the charge carriers which is depend on hopping mechanism. As the voltage increases, the mobility of the hopping ions increases which in turn increases the conductivity of the material [28]. If increase the iron content in the sample, the oxygen vacancies increased. This results increases the free electrondensity and conductivity of the material.

Conclusion

$LaMn_{1-x}Fe_xO_3$ perovskite was synthesized by the co-precipitation method. The XRD pattern confirmed the formation of perovskite phase and the lattice parameters are calculated. The SEM micrographs indicated that the porosity due to inter-particle voids and agglomerated crystals. The presence of La was confirmed by EDX analysis. FTIR spectrum determines the various functional groups present in the compound. The optical band gap decrease with increasing the content of iron in the sample. The conductivity study confirmed that the conductivity increases with increasing the content of iron.

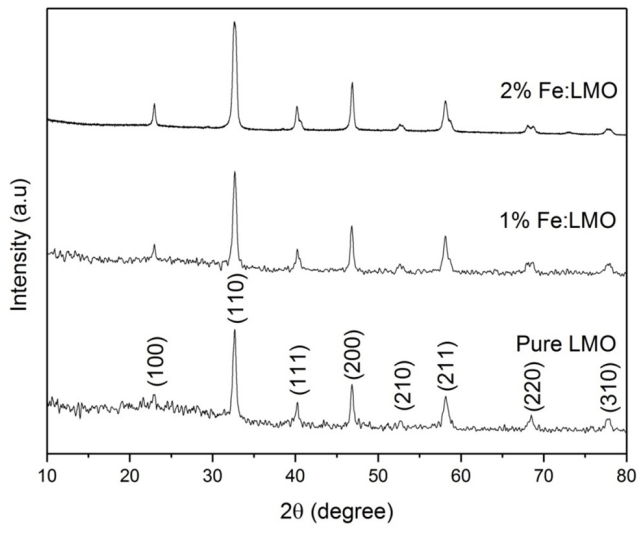

Figure 1: XRD pattern of $LaMn_{1-x}Fe_xO_3$ ($0 \le x \le 0.2$) nanoparticle.

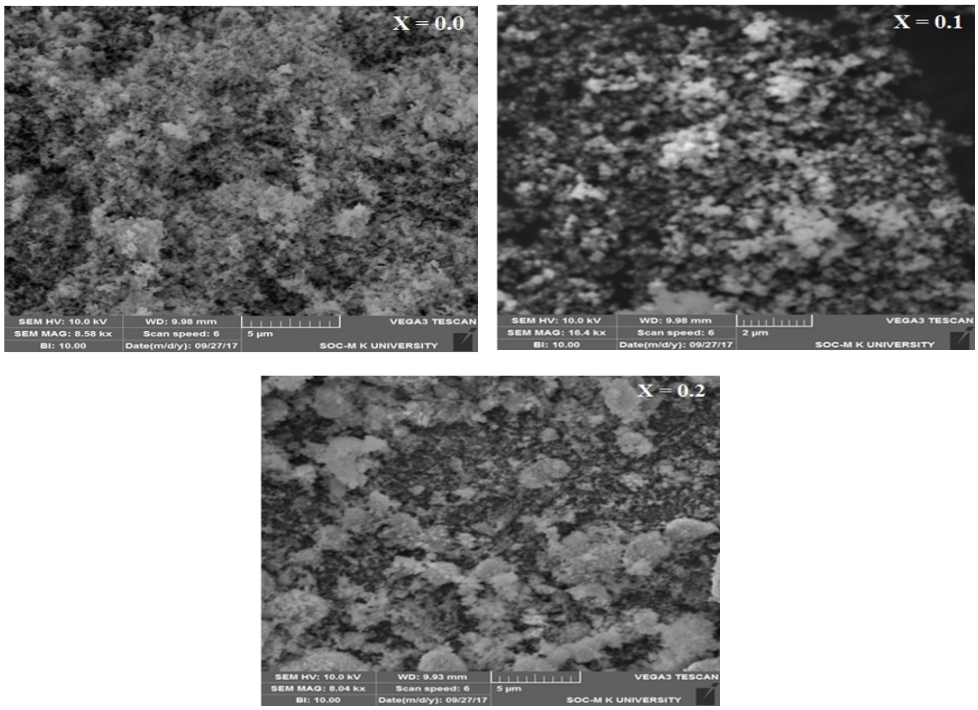

Figure 2: SEM images of $LaMn_{1-x}Fe_xO_3$ ($0 \le x \le 0.2$) nanoparticle.

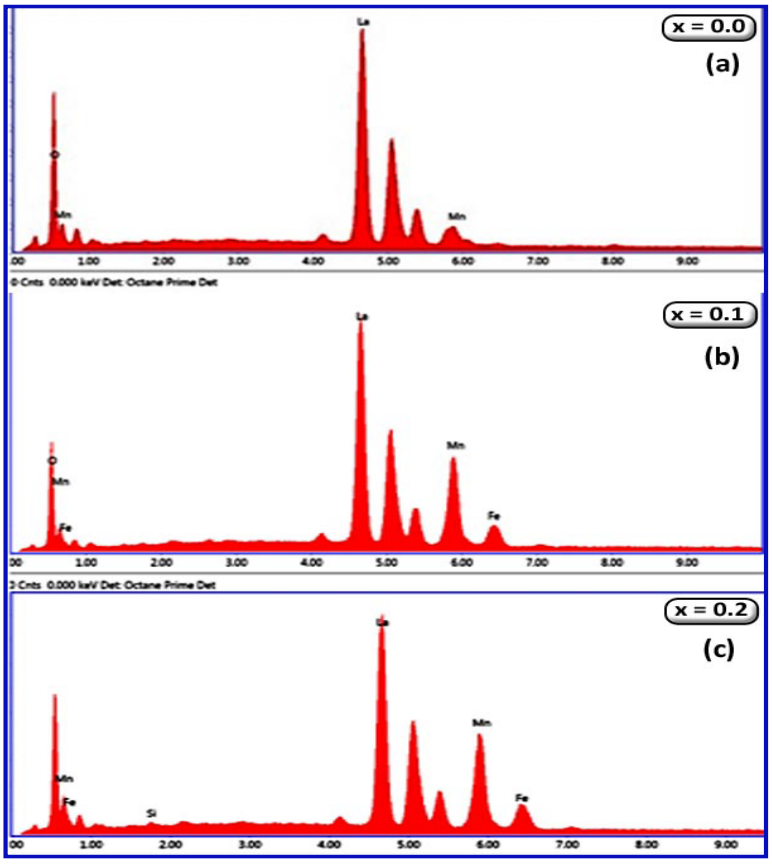

Figure 3: EDAX spectra for $LaMn_{1-x}Fe_xO_3$ ($0 \le x \le 0.2$) nanoparticle.

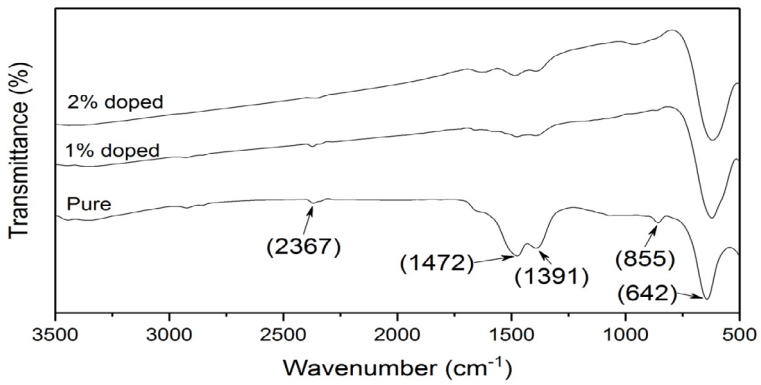

Figure 4: FTIR spectra of $LaMn_{1-x}Fe_xO_3$ ($0 \le x \le 0.2$) nanoparticle.

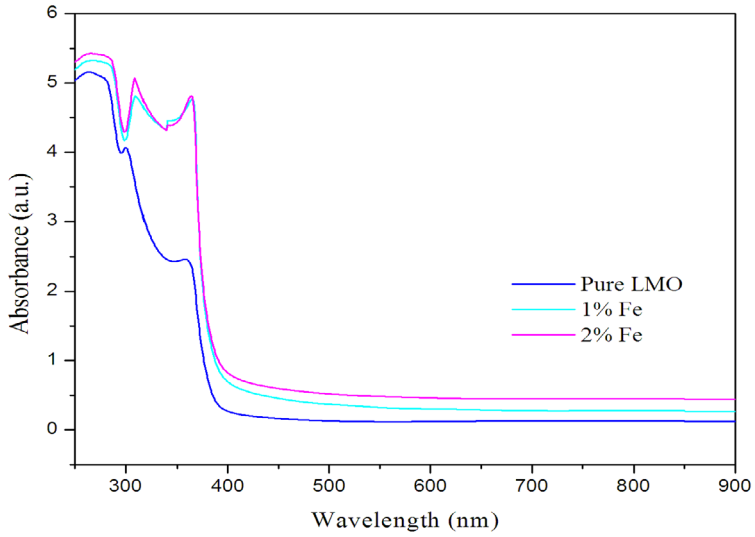

Figure 5a: Absorption spectra of $LaMn_{1-x}Fe_xO_3$ ($0 \le x \le 0.4$) nanoparticle (a) x=0.0 (b) x=0.1 (c) x=0.2.

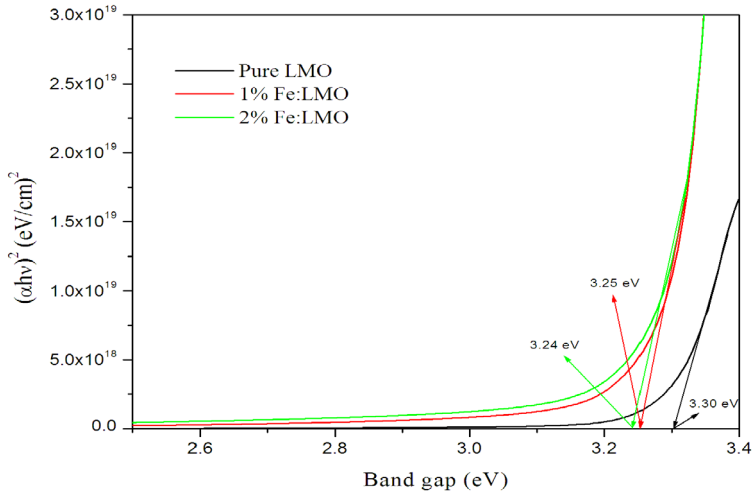

Figure 5b: Plot of $(\alpha h\upsilon)^2$ Vs $(h\upsilon)$ for $LaMn_{1-x}Fe_xO_3$ ($0 \le x \le 0.2$) nanoparticle (a) x=0.0.

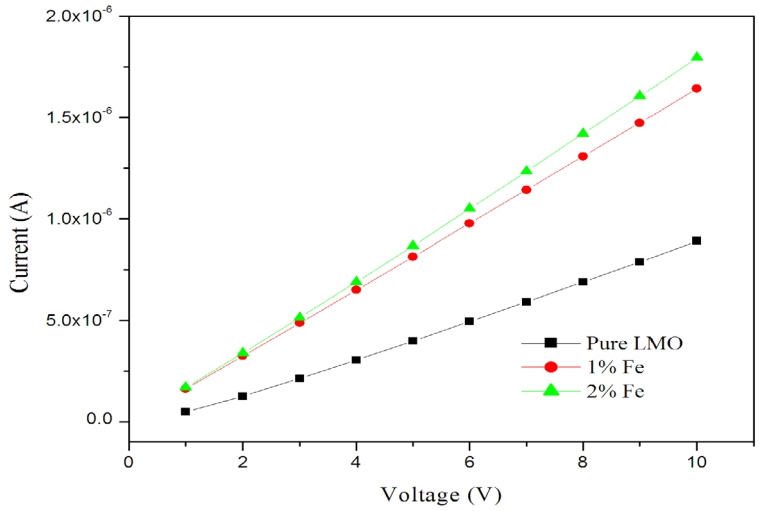

Figure 6: Conductivity spectra for $LaMn_{1-x}Fe_xO_3$ ($0 \le x \le 0.2$) nanoparticle.

S. No	$LaMn_{1-x}Fe_xO_3$ ($0 \le x \le 0.2$)	Lattice Parameter a (Å)	Cell Volume V $(Å)^3$	Crystallite size D (nm)	Dislocation density (10^{15} lines/m^2)	Strain ε (10^{-3} m)
1.	x=0.0	3.8822	58.51048	17.83	3.1443	0.1180
2.	x=0.1	3.8795	58.38849	19.07	2.7481	0.0949
3.	x=0.2	3.8792	58.37494	20.52	2.3746	0.0944

Table 1: Structural parameters of $LaMn_{1-x}Fe_xO_3$ ($0 \le x \le 0.2$) nanoparticle.

$LaMn_{1-x}Fe_xO_3$ ($0 \le x \le 0.2$)	Elemental Composition - Atomic fraction %			
	La	Mn	O	Fe
x=0.0	33.09	3.72	61.61	-
x=0.1	34.58	23.06	35.50	4.57
x=0.2	44.47	36.22	9.91	7.81

Table 2: Compositional analysis for $LaMn_{1-x}Fe_xO_3$ ($0 \le x \le 0.2$) nanoparticle.

S. No	Wave Number (cm^{-1})	Assignment
1	642	Mn-O stretching vibration
2	1391	N-Obending vibration
3	1472	N-Obending vibration
4	2367	O-H Stretching

Table 3: Functional group of $LaMn_{1-x}Fe_xO_3$ ($0 \le x \le 0.2$) nanoparticle.

S. NO	$LaMn_{1-x}Fe_xO_3$ ($0 \le x \le 0.2$)	Band gap (eV)
1	x=0	3.30
2	x=0.1	3.25
3	x=0.2	3.24

Table 4: Bandgap values of $LaMn_{1-x}Fe_xO_3$ ($0 \le x \le 0.2$) nanoparticle.

References

1. Ahmad T, Lone IH, Ubaidullah M, Coolhan K (2013) Low-temperature synthesis, structural and magnetic properties of self-dopant $LaMnO_{3+\delta}$ nanoparticles from a metal-organic polymeric precursor. Mater Res Bull 48: 4723-4728.
2. Krishnamoorthy C, Sethupathi K, Sankaranarayanan V (2007) Magnetic and magneto transport properties of Ce doped nanocrystalline $LaMnO_3$. J Alloy Compd 438: 1-7.
3. Mahmood A, Warsi MF, Ashiq MN, Sher M (2012) Improvements in electrical and dielectric properties of substituted multiferroic $LaMnO_3$ based nanostructures synthesized by co-precipitation method. Mater Res Bull 47: 4197-4202.
4. Kulandaivelu P, Sakthipandi K, Kumar PS, Rajendran V (2013) Mechanical properties of bulk and nanostructured $La_{0.61}Sr_{0.39}MnO_3$ perovskite manganite materials. J Phys Chem Solids 74: 205-214.
5. Tanasescu S, Marinescu C, Maxim F, Raita O (2006) Thermodynamic properties and spin dynamics of some micro and nanostructured magneto resistive lanthanum manganites. J Eur Ceram Soc 26: 3005-3010.
6. Pena M, Fierro J (2001) Chemical structures and performance of perovskite oxides. J Chem Rev 101: 1981-2018.
7. Qiwn Z, Fumio S (2001) Effect of Fe2O3 crystallite size on its mechanochemical reaction with La2O3 to form LaFeO3. J Mater Sci 36: 2287-2290.
8. Nakayama S (2001) LaFeO3 perovskite-type oxide prepared by oxide-mixing, co-precipitation and complex synthesis methods. J Mater Sci 36: 5643-5648.
9. Frank J, Xigolin J, Ramon G, Josef M (2004) 57Fe mössbauer spectroscopy study of LaFe1−x Co x O3 (x=0 and 0.5) formed by mechanical milling. Hyperfine interact 156: 335-340.

10. Yi N, Cao Y, Su Y, Dai WL (2005) Nanocrystalline LaCoO3 perovskite particles confined in SBA-15 silica as a new efficient catalyst for hydrocarbon oxidation. Journal of Catalysis 230: 249-253.

11. Stephan K, Hackenberger M, Kiessling D, Wendt G (2004) Total oxidation of methane and chlorinated hydrocarbons on zirconia supported A1–xSrxMnO3 catalysts. Chemical Engineering and Technology 27: 687-693.

12. Lee YN, Lago RM, Fierro JLG (2001) Surface properties and catalytic performance for ethane combustion of La1−xKxMnO3+δ perovskites. Applied Catalysis A: General. 207: 17-24.

13. Lago RM, Moura FCC, Araujo MH (2007) Investigation of the solid state reaction of LaMnO3 with Feo and its effect on the catalytic reactions with H_2O_2. Journal of the Brazilian Chemical Society. 18: 322-329.

14. Popa M, Frantti J, Kakihana M (2002) Lanthanum ferrite LaFeO3+d nanopowders obtained by the polymerizable complex method. Solid State Ionics 154: 437-445.

15. Lee YN, Lago RM, Fierro JLG, Gonzalez J (2001) Hydrogen peroxide decomposition over Ln1−xAxMnO3 (Ln=La or Nd and A=K or Sr) perovskites. Applied Catalysis 215: 245-256.

16. Athayde DD, Souza DF, Silva AMA, Vasconcelos D (2016) Review of perovskite ceramics synthesis and membrane preparation methods. Ceramics International 42: 6555-6571.

17. Rodriguez DS, Wada H, Yamaguchi S, Farjas J (2017) Synthesis of $LaFeO_3$ perovskite-type oxide via solid-state combustion of a cyano complex precursor: The effect of oxygen diffusion. Ceramics International. 43: 3156-3165.

18. Cao E, Yang Y, Cui T, Zhang Y (2017) Effect of synthesis route on electrical and ethanol sensing characteristics for $LaFeO_{3-\delta}$ nanoparticles by citric solgel method. Applied Surface Science 393: 134-143.

19. Varshney D, Dodiya N, Shaikh MW (2011) Structural properties and electrical resistivity of Na-substituted lanthanum manganites: La1−xNaxMnO3+y (x=0.1, 0.125 and 0.15). J Alloys Compd 509: 7447-7457.

20. Mansuri I, Varshney D (2012) Structure and electrical resistivity of La1−xBaxMnO3 (0.25 ≤ x ≤ 0.35) perovskites. J Alloys Compd 513: 256-265.

21. Cheikh W, Koubaa M, Cheikhrouhou A (2009) Effect of potassium doping on the structural, magnetic and magnetocaloric properties of La0.7Sr0.3−xKxMnO3 perovskite manganites. J Alloys Compd 470: 42-46.

22. Wang H, Zhang X, Hundley MF (2004) Effect of crystallinity on the transport properties of Nd0.67Sr0.33MnO3 thin films. Appl Phys Lett 84: 1147.

23. Tan G, Zhang X, Chen Z (2004) Colossal magnetoresistance effect of electron-doped manganese oxide thin film La1−xTexMnO3(x=0.1,0.15). J Appl Phys 95: 6322.

24. Jin H, Gladden JR, Hu YF (2003) Measurements of elastic constants in thin films of colossal magnetoresistance material. Phys Rev Lett 90: 036103.

25. Coey JMD, Viret M, Molnar SV (1999) Mixed-valence manganites. Adv Phys 48: 167-293.

26. Roy S, Guo YQ, Venkatesh S, Ali N (2001) Interplay of structure and transport properties of sodium-doped lanthanum manganite. J Phys Condens Matter 13: 9547.

27. Urushibara A, Moritomo Y, Arima T (1995) Insulator-metal transition and giant magnetoresistance in La 1−xSrxMnO3. Phys Rev B 51: 14103.

28. Malavasi L, Mozzati M C, Ghigna P, Azzoni CB (2003) Lattice disorder, electric properties, and magnetic behavior of La1-xNaxMnO3+δ manganites. J Phys Chem B 107: 2500-2505.